



**HAL**  
open science

## **AFM imaging of functionalized double-walled carbon nanotubes**

Constanze Lamprecht, Jürgen Danzberger, Petar Lukanov, Carmen-Mihaela Tîlmaciu, Anne-Marie Galibert, Brigitte Soula, Emmanuel Flahaut, Hermann J. Gruber, Peter Hinterdorfer, Andreas Ebner, et al.

► **To cite this version:**

Constanze Lamprecht, Jürgen Danzberger, Petar Lukanov, Carmen-Mihaela Tîlmaciu, Anne-Marie Galibert, et al.. AFM imaging of functionalized double-walled carbon nanotubes. *Ultramicroscopy*, 2009, 109 (8), pp.899-906. 10.1016/j.ultramic.2009.03.034 . hal-03566537

**HAL Id: hal-03566537**

**<https://hal.science/hal-03566537>**

Submitted on 11 Feb 2022

**HAL** is a multi-disciplinary open access archive for the deposit and dissemination of scientific research documents, whether they are published or not. The documents may come from teaching and research institutions in France or abroad, or from public or private research centers.

L'archive ouverte pluridisciplinaire **HAL**, est destinée au dépôt et à la diffusion de documents scientifiques de niveau recherche, publiés ou non, émanant des établissements d'enseignement et de recherche français ou étrangers, des laboratoires publics ou privés.



## Open Archive Toulouse Archive Ouverte (OATAO)

OATAO is an open access repository that collects the work of Toulouse researchers and makes it freely available over the web where possible.

This is an author-deposited version published in: <http://oatao.univ-toulouse.fr/>  
Eprints ID: 3790

**To link to this article:** doi:10.1016/j.ultramic.2009.03.034  
URL <http://dx.doi.org/10.1016/j.ultramic.2009.03.034>

To cite this version: Lamprecht, C. and Danzberger, J. and Lukanov, P. and Trîlmaciu, C-M and Galibert, Anne Marie and Soula, Brigitte and Flahaut, Emmanuel and Gruber, H.J and Hinterdorfer, P. and Ebner, A. and Kienberger, F. ( 2009) *AFM imaging of functionalized double-walled carbon nanotubes*. Ultramicroscopy, vol.109 (8). pp. 899-906. ISSN 0304-3991

Any correspondence concerning this service should be sent to the repository administrator: [staff-oatao@inp-toulouse.fr](mailto:staff-oatao@inp-toulouse.fr)

# AFM imaging of functionalized double-walled carbon nanotubes

C. Lamprecht<sup>a</sup>, J. Danzberger<sup>a</sup>, P. Lukanov<sup>b</sup>, C.-M. Tîlmaciu<sup>b</sup>, A.-M. Galibert<sup>b</sup>, B. Soula<sup>b</sup>, E. Flahaut<sup>b</sup>, H.J. Gruber<sup>a</sup>, P. Hinterdorfer<sup>a</sup>, A. Ebner<sup>a,\*</sup>, F. Kienberger<sup>a,c,\*\*</sup>

<sup>a</sup> Institute of Biophysics, J. Kepler University, Altenbergerstraße 69, A-4040 Linz, Austria

<sup>b</sup> Université de Toulouse, CIRIMAT, UPS/INPT/CNRS, 31062 Toulouse Cedex 9, France

<sup>c</sup> Agilent Laboratories Linz, Aubrunnerweg 11, A-4040 Linz, Austria

## A B S T R A C T

We present a comparative study of several non-covalent approaches to disperse, debundle and non-covalently functionalize double-walled carbon nanotubes (DWNTs). We investigated the ability of bovine serum albumin (BSA), phospholipids grafted onto amine-terminated polyethylene glycol (PL-PEG<sub>2000</sub>-NH<sub>2</sub>), as well as a combination thereof, to coat purified DWNTs. Topographical imaging with the atomic force microscope (AFM) was used to assess the coating of individual DWNTs and the degree of debundling and dispersion. Topographical images showed that functionalized DWNTs are better separated and less aggregated than pristine DWNTs and that the different coating methods differ in their abilities to successfully debundle and disperse DWNTs. Height profiles indicated an increase in the diameter of DWNTs depending on the functionalization method and revealed adsorption of single molecules onto the nanotubes. Biofunctionalization of the DWNT surface was achieved by coating DWNTs with biotinylated BSA, providing for biospecific binding of streptavidin in a simple incubation step. Finally, biotin-BSA-functionalized DWNTs were immobilized on an avidin layer via the specific avidin-biotin interaction.

## 1. Introduction

Due to their remarkable electronic, mechanical, chemical and thermal properties CNTs have turned out to be nanodevices with a wide range of potential applications in various composite materials, technical devices [1,2], as well as medical and pharmaceutical products [3,4]. Double-walled carbon nanotubes (DWNTs) are of special interest as they bridge the gap between single-walled carbon nanotubes (SWNTs) and the more complex multi-walled carbon nanotubes (MWNTs). DWNTs are comparable to SWNTs with respect to their small diameter, yet their mechanical stability is much higher than that of SWNTs. Moreover, the outer wall can be functionalized without changing the mechanical and electronic properties of the inner nanotube [5]. These properties make them attractive for biological and biomedical applications. However, DWNTs, as all pristine CNTs, have a strong tendency to aggregate and are practically insoluble in any kind of solvent because of substantial van der Waals attractions among them. Solubility in aqueous media, however, is

a fundamental prerequisite for potential biological and biomedical applications. Several strategies have been explored to disperse and solubilize CNTs which can be divided into two main categories. One approach is based on covalent CNT functionalization by cutting and oxidizing CNTs. Thus, carboxylic groups are generated which are subsequently derivatized with different types of molecules [6–10]. The second dispersal method is the non-covalent coating of CNTs [11] with surfactants molecules [12–14], nucleic acids [15–17], proteins and peptides [18–21], or polymers [22–27]. The non-covalent dispersion procedures usually involve ultrasonication, centrifugation and filtration. They are quick and easy, achieving debundling of CNTs, dispersion in water and biocompatibility in one step.

In this study we present a comparative investigation of non-covalent approaches to debundle, disperse and functionalize DWNTs. We used bovine serum albumin (BSA) and a phospholipid-linked polyethylene glycol chain with a terminal amino group (PL-PEG-NH<sub>2</sub>), as well as a combination thereof, to coat purified DWNTs. Topographical atomic force microscope (AFM) imaging was used for the direct assessment of a successful functionalization procedure and proved that functionalized DWNTs are better separated and less aggregated than pristine DWNTs. We demonstrate the ability of the non-covalent functionalization scheme to provide DWNTs for specific recognition by, and binding of biomolecules, using the well-studied biotin/avidin and biotin/

Corresponding author.

Corresponding author at: Agilent Laboratories Linz, Aubrunnerweg 11, A-4040 Linz, Austria.

E-mail addresses: andreas.ebner@jku.at (A. Ebner), ferry\_kienberger@agilent.com (F. Kienberger).

streptavidin interaction [28]. We present high-resolution topographical images of functionalized DWNTs captured onto a dense avidin layer in aqueous buffer solution. To our knowledge, this is the first successful attempt to image single functionalized carbon nanotubes in liquid under physiological conditions using AFM.

## 2. Materials and methods

### 2.1. Preparation and purification of double-walled carbon nanotubes

Synthesis and purification of double-walled carbon nanotubes used for the experiments are explained in detail elsewhere [5]. Briefly, DWNTs were synthesised by catalytic chemical vapour deposition (CCVD), the catalyst being an  $Mg_{1-x}Co_xO$  solid solution containing added Mo oxide. The MgO-based catalyst was removed by thorough washing with HCl solution. The extracted powder contained only clean carbon nanotubes of which ~80% are DWNTs and the rest being SWNTs (15%) and triple-walled CNTs (5%). HRTEM observation showed a variation of outer diameter from 1.2 to 3.2 nm. The median outer diameter is 2.0 nm.

### 2.2. Non-covalent functionalization of DWNTs with BSA

Purified DWNTs and BSA (Roche) were mixed with ultra-pure water with a concentration of 0.25 and 1.0 mg/ml, respectively. The mixture was sonicated for 45 min (Bandelin Sonoplus GM70 at 20% power) under cooling in an ice bath. The procedure resulted in a stable black suspension. The DWNT BSA suspension was then filtered in centrifugation cartridges with ultrafiltration membranes (nanosep, 300 kD cutoff) at around 5500g (Eppendorf Centrifuge 5417C) and washed 5 times with ultra-pure water to remove excess BSA. After re-suspension in ultra-pure water the concentration of DWNTs was estimated to be 0.05–0.1 mg/ml due to loss of material at the sidewall of the filtration device and the filter membrane. The suspension was stored at 4 °C until further usage within the next 2–3 days.

### 2.3. Phospholipids (PL) grafted on polyethylene glycol (PEG)

PL-PEG-NH<sub>2</sub> (2-distearoyl-*sn*-glycero-3-phosphoethanolamine-*N*-[amin(PEG)2000], Avanti Polar Lipids) was used at a concentration of 1 mg/ml to suspend DWNTs at a concentration of 0.25 mg/ml in water using a similar sonication, filtration and washing procedure as described for BSA coating. The speed of the centrifuge was adjusted to 7000g for filtration and washing. The

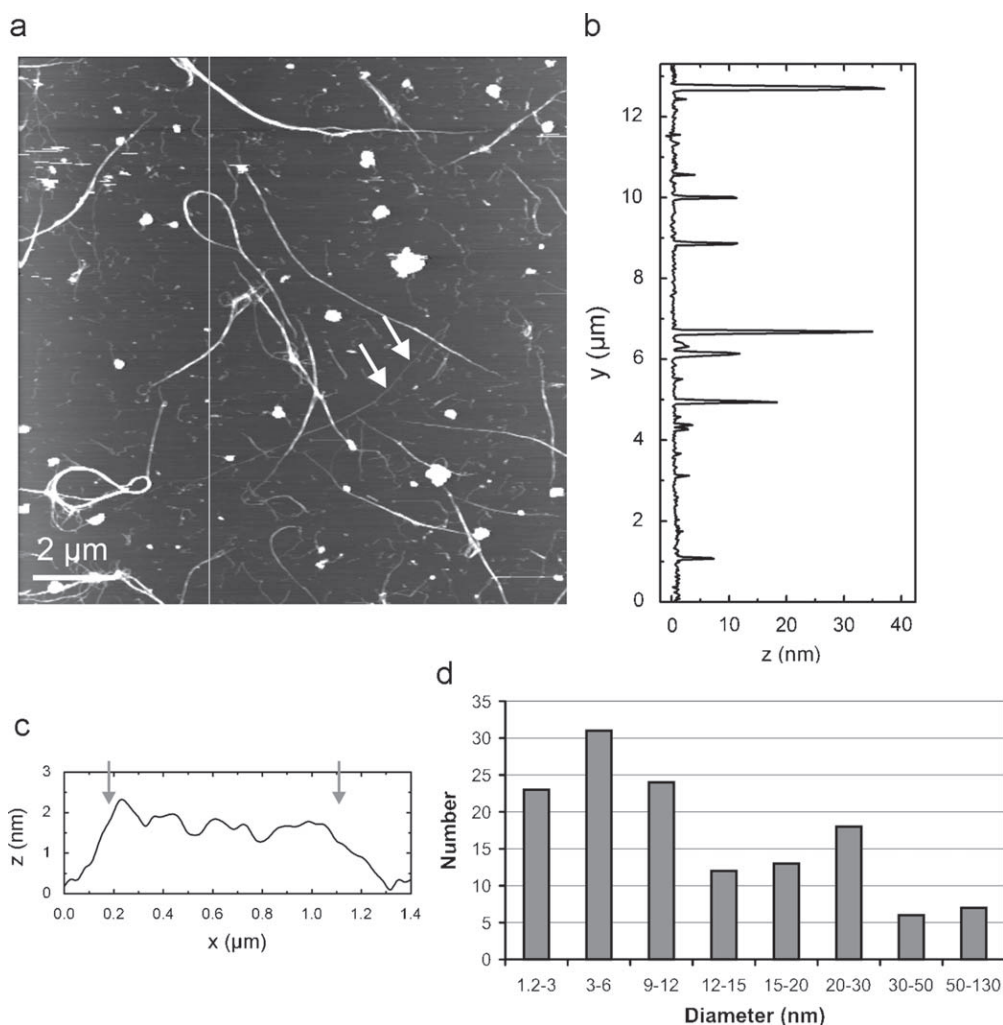


**Fig. 1.** Non-functionalized DWNTs. (a) Topographical image of DWNTs deposited on mica after immersion in 1,2-dichloroethane. The length of bundles varied between several 100 nm and 20 μm. (b) Height profile along the white line in (a). (c) Cross-section profile along a pristine CNT. Arrows mark corresponding positions in (a). (d) Height distribution of non-functionalized DWNTs.

final PL-PEG/DWNT suspension had an estimated concentration of around 0.2 mg/ml due to loss of material in the filter device.

#### 2.4. Conjugation of BSA and PL-PEG to DWNTs

Purified DWNTs were added to a 5  $\mu$ M aqueous solution of BSA at a final concentration of 0.25 mg/ml and sonicated under cooling for 45 min. Subsequently, PL-PEG-NH<sub>2</sub> was added to the suspension at a concentration of 0.5 mg/ml. The mixture was sonicated for an additional period of 45 min under cooling. The suspension was filtered by centrifugation through an ultrafiltration membrane (300 kD cutoff) at 7000g to remove excess BSA and PEG-lipids. The BSA and PL-PEG DWNT conjugates were washed and re-suspended in ultra-pure water at a final concentration of around 0.2 mg/ml and stored at 4 °C.

#### 2.5. Biotinylated BSA

Biotin-IgG was prepared similarly as described by Kamruzzahan et al. [28]. 5 mg (33 nmol) goat IgG purchased from Sigma was

dissolved in 0.5 ml buffer (100 mM NaCl, 35 mM boric acid, pH adjusted to 8.5 using NaOH) and 5  $\mu$ l of 66 mM biotin-cap-NHS [29] in DMSO were slowly added while gentle vortexing. After 30 min reaction time (with occasional gentle vortexing) the biotinylated IgG was purified using gel filtration [26]. The functionalization of DWNTs with biotinylated BSA was done using the same procedure as described above for BSA/DWNTs. The filtered and washed functionalized DWNTs were re-suspended either in ultra-pure water or in 0.1  $\times$  PBS, a 9/1 mixture (v/v) of water and phosphate-buffered saline (PBS, 150 mM NaCl, 5 mM NaH<sub>2</sub>PO<sub>4</sub>, pH = 7.4 adjusted with NaOH).

#### 2.6. Incubation of biotin-BSA/DWNTs with streptavidin

Thirty microlitres of streptavidin with a concentration of 1.3 mg/ml was added to 3.5 ml aqueous suspension of biotin-BSA-functionalized DWNTs at a concentration of around 0.2 mg/ml. The mixture was filtered and washed after 1 h of incubation (nanosep, 300 kD cutoff) to remove excess streptavidin. The

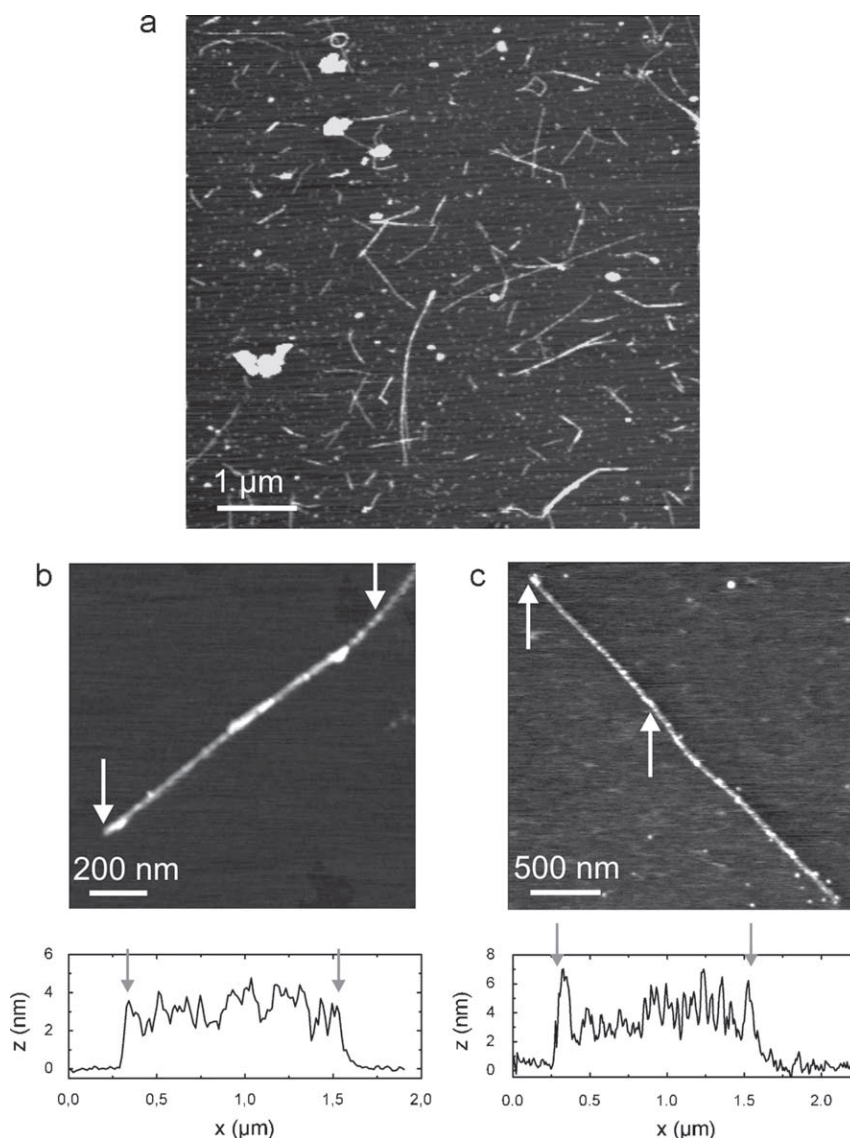


**Fig. 2.** Topographical images of BSA-coated DWNTs on mica obtained by contact mode imaging in air. (a) Survey scan showing mostly single and well-separated DWNTs. (b) and (c) Images of individual DWNTs with bright dot-like structures potentially representing single BSA molecules. White arrows mark corresponding positions in the cross-section profiles below.

remaining functionalized nanotubes were re-suspended in ultra-pure water and stored at 4 °C.

### 2.7. Preparation of avidin layer and incubation with biotin-BSA/DWNTs

In order to prepare a dense layer of avidin molecules for incubation with biotin-BSA-functionalized DWNTs, a stock solution of avidin (1 mg/ml in PBS) was diluted with 9 volumes of water to adjust a final avidin concentration of 0.1 mg/ml. Freshly cleaved muscovite mica was mounted in a commercial AFM fluid cell prior to AFM imaging and incubated with the diluted avidin solution. The avidin molecules are immobilized onto mica via electrostatic adsorption due to their positive net charge [26]. After 20 min the mica sheet was extensively rinsed with 0.1 × PBS. Finally, the fluid cell was filled with 600 μl of a biotin-BSA/DWNTs suspension in 0.1 × PBS at a concentration of 0.2 mg/ml. The fluid cell was allowed to stand for 20 min. Before starting AFM imaging

the biotin-BSA/DWNTs suspension was removed and exchanged for 0.1 × PBS.

### 2.8. Contact mode AFM imaging

For atomic force microscope imaging of purified DWNTs, a small amount of the powdered sample was dispersed in 1,2-dichloroethane (DCE) under strong sonication (Bandelin Sonoplus GM70 at 50% power) in 3 cycles with 30 s sonication time each. A 10 μl droplet was placed on freshly cleaved mica substrate immediately after sonication. For topographical imaging of biomolecule conjugated DWNTs samples were prepared by placing a 5–10 μl droplet on freshly cleaved mica substrate and allowing it to dry. Imaging was done with a Nanoscope IIIa (Digital Instruments, Santa Barbara, CA) or a PicoSPM setup (Agilent Technologies, Chandler, AZ) operated in contact mode at room temperature with a lateral scan rate of 1–1.5 Hz at 512 lines. AFM cantilevers with a nominal spring constant of 0.01–0.03 N/m were

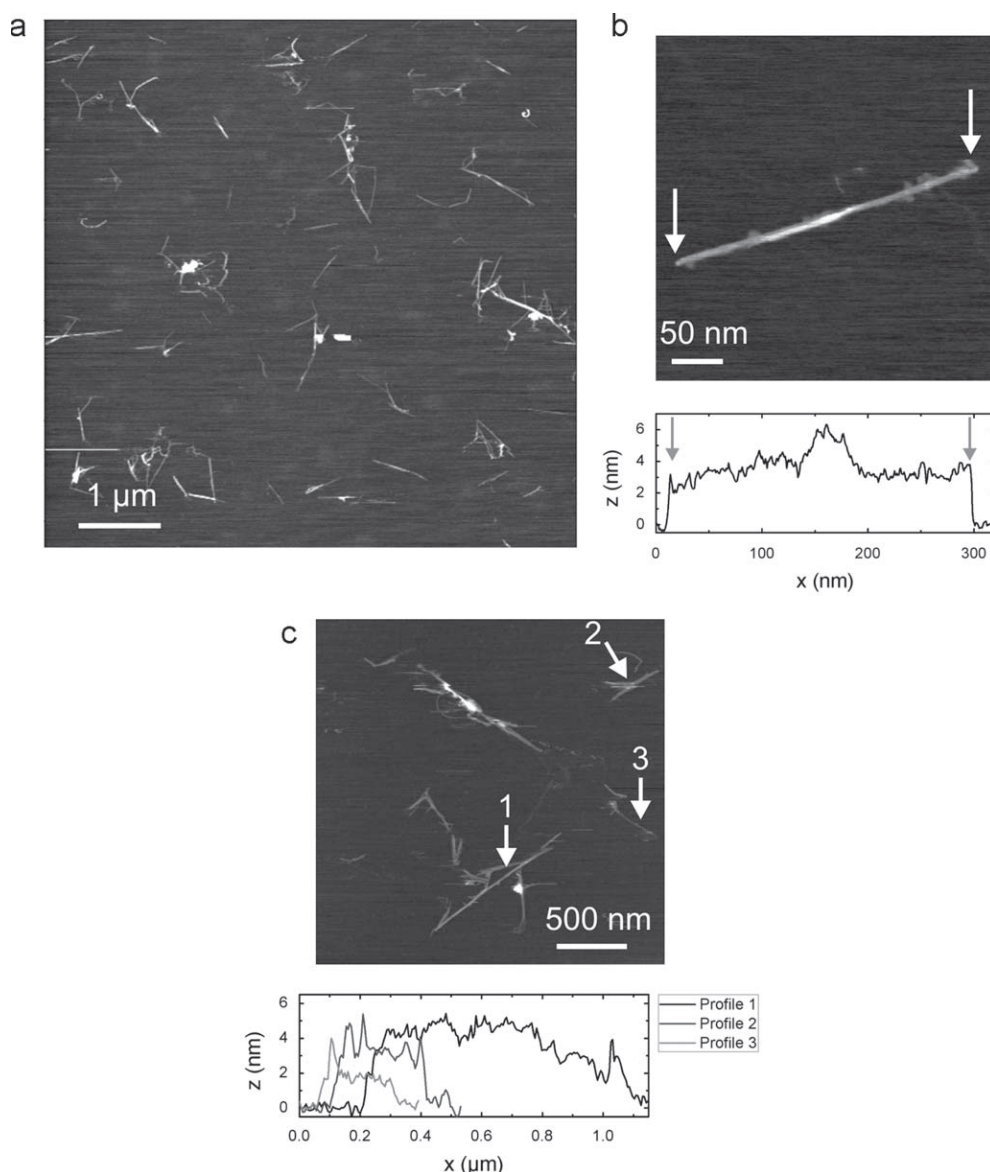


**Fig. 3.** Topographical images of DWNTs covered with PL-PEG<sub>2000</sub>-NH<sub>2</sub>. (a) Overview scan showing well-separated and individual DWNTs. (b) and (c) Images and cross-section profiles of individual PL-PEG-coated DWNTs. Arrows mark positions in the corresponding cross-section profile. Arrows with numbers refer to corresponding profiles.

used. Each functionalization procedure was repeated 2–4 times and at least 2 samples were taken for AFM evaluation.

### 2.9. MAC mode imaging

Topographical imaging of biotin-BSA/DWNTs incubated on an avidin layer was carried out in PBS at room temperature. Images were acquired with a magnetically driven dynamic force microscope (MACmode, Agilent Technologies, Chandler, AZ) equipped with a conventional fluid cell. AFM tips with magnetic coating (Agilent Technologies, Chandler, AZ) and nominal spring constant of 0.1 N/m were used. The measurement frequency was set to 20% below the resonance frequency. Scanning was done with the feedback adjusted to 40% amplitude reduction at a lateral scan frequency of 1.0 Hz with 512 scan lines per image.

## 3. Results and discussion

### 3.1. Topographical imaging of functionalized DWNTs

Fig. 1a shows a survey image of non-functionalized DWNTs after immersion in the organic solvent DCE and subsequent evaporation revealing aggregates and long bundles of different height and length. Cross-sectional analysis (Fig. 1b and d) revealed that most DWNTs are present as bundles ranging from 2 to 130 nm in height and few micrometers in length. From cross-section profiles taken on non-functionalized DWNTs the height variance was observed to be  $\sim 0.5$  nm (Fig. 1c). Because of their hydrophobic nature, many individual DWNTs aggregate and form rope-like structures when the organic solvent is evaporated [30–32].

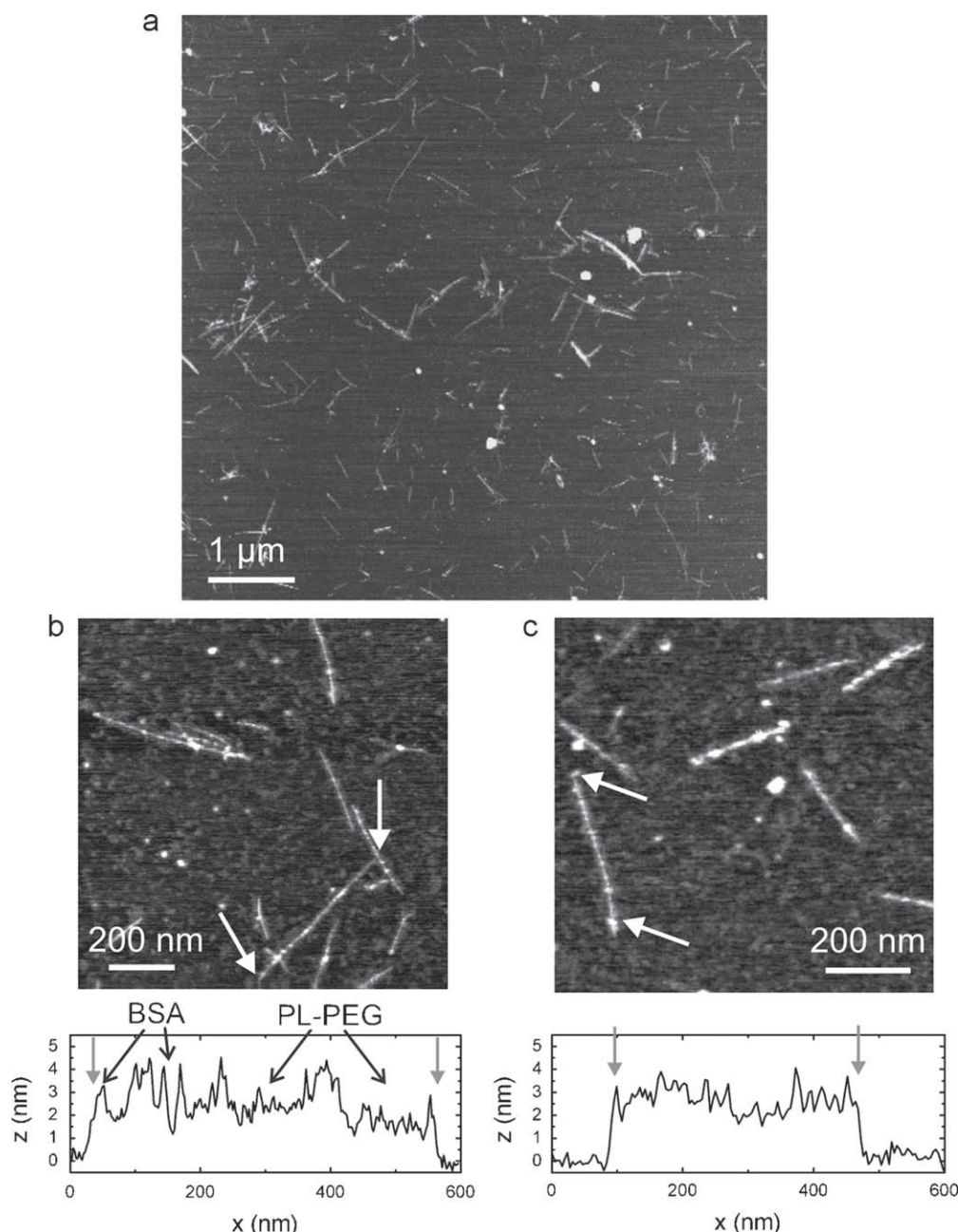


**Fig. 4.** Topographical images of bi-conjugated DWNTs using BSA and PL-PEG<sub>2000</sub>-NH<sub>2</sub>. (a) Overview scan. (b) and (c) Small scan size images with corresponding cross-section profiles. Peaks in the cross-section profile suggest the adsorption of BSA while flat and amorphous segments indicate adsorption of PL-PEG<sub>2000</sub>-NH<sub>2</sub>. White arrows in the images mark the positions where cross-section profiles were acquired.

Topographical images of an aqueous dispersion of BSA-DWNTs are shown in Fig. 2. In contrast to un-modified DWNTs, the majority of BSA-DWNTs were found to be well dispersed as separated individual tubes (Fig. 2a). Bright dot-like structures covering individual DWNTs were observed (Fig. 2b and c). From the cross-section profiles along the tubes peak heights of 1–2 nm were obtained, suggesting the adsorption of single BSA molecules, whereas peaks of up to 5 nm in height indicated BSA multimers attached to DWNTs. Recent studies on the adsorption of BSA and HSA on carbon nanotubes showed that the adsorption is driven by hydrophobic and electrostatic interactions [33,34].

Fig. 3a shows an overview scan of an aqueous dispersion of PL-PEG-modified DWNTs (phospholipids grafted on polyethylene glycol) with well-separated and mostly individual nanotubes. Small scan size images (Fig. 3b and c) reveal that DWNTs are uniformly wrapped with PL-PEG along the entire length of the nanotube. The average height of PL-PEG-functionalized DWNTs is ~3 nm, with peak heights of 6 nm (Fig. 3b, lower panel). In Fig. 3c the height profiles of three different tubes are

compared with step sizes of ~1 nm, which is the expected thickness of PL-PEG coating.

Fig. 4 shows DWNTs dispersed with both BSA and PL-PEG (DSPE-PEG<sub>2000</sub>-NH<sub>2</sub>). Again, short and individual DWNTs appeared well separated. In small scan size images (Fig. 4b and c) BSA was observed as dot-like structures on the nanotube surface but was found not to cover the entire DWNT. Also, segments with uniform and soft appearing features were visible on the DWNTs suggesting the adsorption of PL-PEG. The immobilization of both BSA and PL-PEG on the same DWNT indicates a bi-conjugation of DWNT with BSA and PEG grafted phospholipids. The cross-section profile indeed showed segments with distinct peaks (~2 nm above the DWNT baseline) together with a rather uniform height distribution (~1 nm above the baseline) corresponding to BSA and PL-PEG, respectively. Although the separation of DWNTs worked properly with either BSA or PL-PEG, the joint bi-functionalization with both BSA and PL-PEG resulted in the most efficient debundling and separation of DWNTs, as judged from the long-term stability in solution and from topographical AFM images.

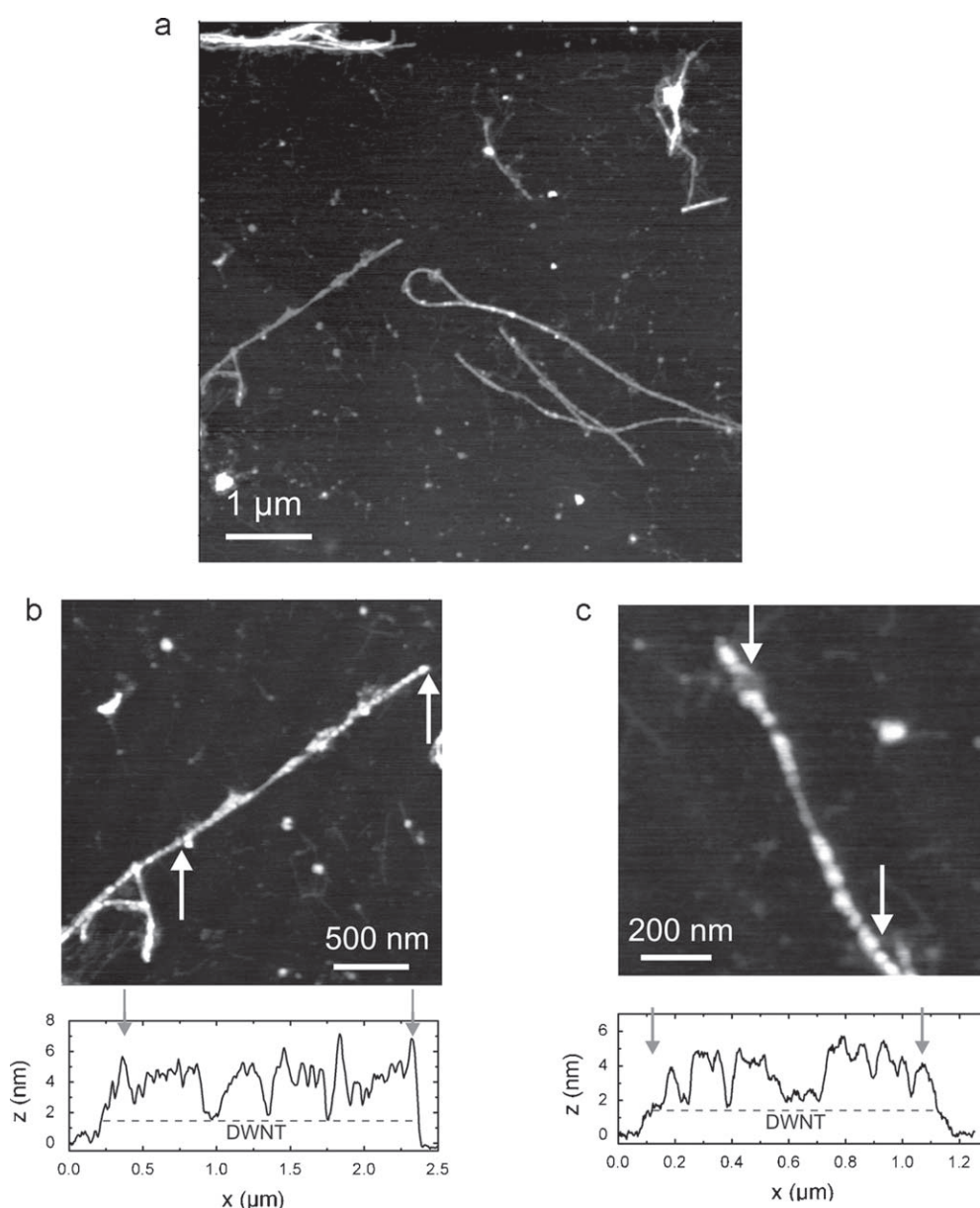


**Fig. 5.** Specific binding of streptavidin to biotin-BSA-functionalized DWNTs. (a) Overview scan showing separated and individual nanotubes. (b) and (c) Small scan size images and corresponding cross-section profiles. Arrows in the images mark positions where the cross-section profiles were acquired.

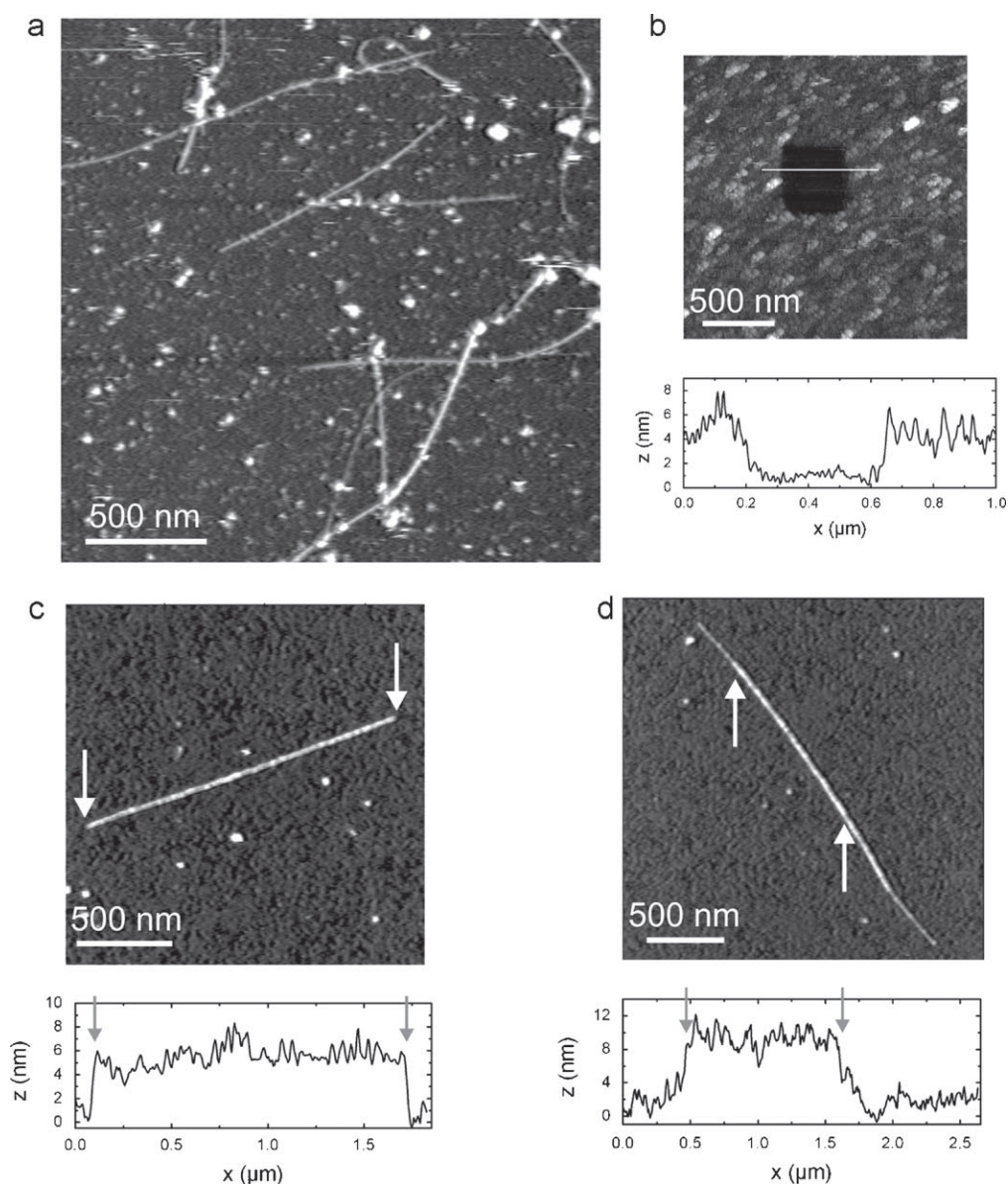


**Fig. 6.** Specific immobilization of biotin-BSA-functionalized DWNTs to a dense layer of avidin on mica. (a) Overview image of several biotin-BSA DWNTs bound to the avidin layer. (b) A rectangular hole was scratched into the avidin layer and imaged subsequently. From the cross-section profile the layer height was determined to be  $\sim 4$  nm. (c) and (d) Small scan size images and cross-section profiles of single biotin-BSA DWNTs specifically bound to the avidin layer.

### 3.2. Specific binding of functionalized DWNTs

For testing specific binding of biomolecules to functionalized DWNTs we used biotinylated BSA for functionalization of DWNTs (biotin-BSA DWNTs) and subsequent exposure to a solution of streptavidin. After filtering and washing of the streptavidin containing suspension of biotin-BSA DWNTs, a droplet of the dispersion was placed on mica and allowed to dry. Fig. 5 shows topographical images with dot-like features decorating most of the DWNTs over the entire length, indicating dense coating with molecules. The corresponding height profile analysis (Fig. 5b and c) showed a peak height of 3–4 nm above the DWNT baseline (with 1–2 nm height of biotinylated BSA alone), indicating that streptavidin had covered most of the biotin BSA functionalized nanotube surface.

For specific and tight immobilization of DWNTs we prepared a dense layer of avidin with subsequent incubation of biotin-BSA DWNTs in buffer solution for 20 min. The sample was rigorously washed to remove loosely bound DWNTs. Fig. 6 shows

topographical images of biotin-BSA DWNTs on a dense layer of avidin. The intactness of the avidin layer was proven by scratching experiments resulting in a layer height of  $\sim 4$  nm (Fig. 6b). Small scan size images and corresponding cross-section profiles (Fig. 6b and c) again show that the entire DWNTs were covered by bright dots representing biotin-BSA adsorbed to the nanotubes. Due to the strong and specific interaction between biotin-BSA DWNTs and the mica-bound avidin layer, the nanotubes were easily imaged in liquid conditions without any tip-induced movements.

## 4. Conclusion

We have established simple functionalization procedures that provide stable aqueous suspensions of debundled and individual DWNTs using BSA, PL-PEG or a combination thereof. AFM topographical imaging was used for a simple and direct assessment of bundling and aggregation of DWNTs, revealing well dispersed and separated DWNTs after proper functionalization.

Biotin-BSA-functionalized DWNTs were shown to specifically bind streptavidin, moreover biotin-BSA DWNTs could be specifically and tightly immobilized to a dense layer of mica-bound avidin. In conclusion, we have demonstrated a successful non-covalent functionalization scheme to modify DWNTs for specific recognition and binding of biomolecules, which may prove to be useful for future use of CNTs in biological applications.

### Acknowledgements

We thank Tuomas Näreoja for technical discussions, Dr. Ruediger Klingeler for supporting materials, and Elena Heister, Vera Neves, Dr. Vanesa Beltran, Dr. Helen Coley and Prof. Johnjoe McFadden for helpful discussions. This work was supported by EC grant Marie Curie RTN-CT-2006-035616, CARBIO 'Carbon nanotubes for biomedical applications'.

### References

- [1] S. Iijima, *Nature* 354 (6348) (1991) 56–58.
- [2] M.S.D. Dresselhaus, Gene, in: Avouris, Phaedon (Eds.), *Carbon Nanotubes: Synthesis, Structure, Properties, and Applications*, vol. 80, Springer, Berlin, Heidelberg, 2001.
- [3] C. Klumpp, K. Kostarelos, M. Prato, A. Bianco, *Biochimica et Biophysica Acta* 1758 (3) (2006) 404–412.
- [4] L. Lacerda, A. Bianco, M. Prato, K. Kostarelos, *Advanced Drug Delivery Reviews* 58 (14) (2006) 1460–1470.
- [5] E. Flahaut, R. Bacsa, A. Peigney, C. Laurent, *Chemical Communications* (12) (2003) 1442–1443.
- [6] J.L. Bahr, J.M. Tour, *Journal of Materials Chemistry* 12 (7) (2002) 1952–1958.
- [7] A. Bianco, K. Kostarelos, C.D. Partidos, M. Prato, *Chemical Communications* (5) (2005) 571–577.
- [8] A. Hirsch, *Angewandte Chemie-International Edition* 41 (11) (2002) 1853–1859.
- [9] J.L. Stevens, A.Y. Huang, H.Q. Peng, L.W. Chiang, V.N. Khabashesku, J.L. Margrave, *Nano Letters* 3 (3) (2003) 331–336.
- [10] N. Tagmatarchis, M. Prato, *Journal of Materials Chemistry* 14 (4) (2004) 437–439.
- [11] S. Singh, P. Kruse, *International Journal of Nanotechnology* 5 (9–12) (2008) 900–929.
- [12] M.F. Islam, E. Rojas, D.M. Bergey, A.T. Johnson, A.G. Yodh, *Nano Letters* 3 (2) (2003) 269–273.
- [13] V.C. Moore, M.S. Strano, E.H. Haroz, R.H. Hauge, R.E. Smalley, J. Schmidt, Y. Talmon, *Nano Letters* 3 (10) (2003) 1379–1382.
- [14] C. Richard, F. Balavoine, P. Schultz, T.W. Ebbesen, C. Mioskowski, *Science* 300 (5620) (2003) 775–778.
- [15] B. Onoa, M. Zheng, M.S. Dresselhaus, B.A. Diner, *Physica Status Solidi a-Applications and Materials Science* 203 (6) (2006) 1124–1131.
- [16] M. Zheng, A. Jagota, E.D. Semke, B.A. Diner, R.S. McLean, S.R. Lustig, R.E. Richardson, N.G. Tassi, *Nature Materials* 2 (5) (2003) 338–342.
- [17] R.R. Lahiji, B.D. Dolash, D.E. Bergstrom, R. Reifenger, *Small* 3 (11) (2007) 1912–1920.
- [18] R.J. Chen, S. Bangsaruntip, K.A. Drouvalakis, N.W. Kam, M. Shim, Y. Li, W. Kim, P.J. Utz, H. Dai, *Proceedings of the National Academy of Sciences of the United States of America* 100 (9) (2003) 4984–4989.
- [19] N.W. Kam, H. Dai, *Journal of the American Chemical Society* 127 (16) (2005) 6021–6026.
- [20] D. Nepal, K.E. Geckeler, *Small* 3 (7) (2007) 1259–1265.
- [21] V. Zorbas, A. Ortiz-Acevedo, A.B. Dalton, M.M. Yoshida, G.R. Dieckmann, R.K. Draper, R.H. Baughman, M. Jose-Yacaman, I.H. Musselman, *Journal of the American Chemical Society* 126 (23) (2004) 7222–7227.
- [22] X. Chen, U.C. Tam, J.L. Czapinski, G.S. Lee, D. Rabuka, A. Zettl, C.R. Bertozzi, *Journal of the American Chemical Society* 128 (19) (2006) 6292–6293.
- [23] N.W.S. Kam, M. O'Connell, J.A. Wisdom, H.J. Dai, *Proceedings of the National Academy of Sciences of the United States of America* 102 (33) (2005) 11600–11605.
- [24] N. Nakayama-Ratchford, S. Bangsaruntip, X.M. Sun, K. Welsher, H.J. Dai, *Journal of the American Chemical Society* 129 (9) (2007) 2448–2449.
- [25] M.J. O'Connell, P. Boul, L.M. Ericson, C. Huffman, Y.H. Wang, E. Haroz, C. Kuper, J. Tour, K.D. Ausman, R.E. Smalley, *Chemical Physics Letters* 342 (3–4) (2001) 265–271.
- [26] P. Petrov, F. Stassin, C. Pagnoulle, R. Jerome, *Chemical Communications* (23) (2003) 2904–2905.
- [27] R. Krajcik, A. Jung, A. Hirsch, W. Neuhuber, O. Zolk, *Biochemical and Biophysical Research Communications* 369 (2) (2008) 595–602.
- [28] A.S.M. Kamruzzahan, A. Ebner, L. Wildling, F. Kienberger, C.K. Riener, C.D. Hahn, P.D. Pollheimer, P. Winklehner, M. Holzl, B. Lackner, D.M. Schorkl, P. Hinterdorfer, H.J. Gruber, *Bioconjugate Chemistry* 17 (6) (2006) 1473–1481.
- [29] M. Wilchek, E.A. Bayer, *Methods in Enzymology* 184 (1990) 123–138.
- [30] M.S. Strano, V.C. Moore, M.K. Miller, M.J. Allen, E.H. Haroz, C. Kittrell, R.H. Hauge, R.E. Smalley, *Journal of Nanoscience and Nanotechnology* 3 (1–2) (2003) 81–86.
- [31] F. Balavoine, P. Schultz, C. Richard, V. Mallouh, T.W. Ebbesen, C. Mioskowski, *Angewandte Chemie-International Edition* 38 (13–14) (1999) 1912–1915.
- [32] M. Shim, N.W.S. Kam, R.J. Chen, Y.M. Li, H.J. Dai, *Nano Letters* 2 (4) (2002) 285–288.
- [33] L.E. Valenti, P.A. Fiorito, C.D. Garcia, C.E. Giacomelli, *Journal of Colloid and Interface Science* 307 (2) (2007) 349–356.
- [34] J.W. Shen, T. Wu, Q. Wang, Y. Kang, *Biomaterials* 29 (28) (2008) 3847–3855.